# SUPPORTING INFORMATION

## Two dynamical regimes of the substrate radical rearrangement reaction in $B_{12}$-dependent ethanolamine ammonia-lyase resolve contributions of native protein configurations and collective configurational fluctuations to catalysis

Meghan Kohne, Chen Zhu, and Kurt Warncke*

*email: kwarncke@physics.emory.edu

## Table of Contents

**1. Supporting Methods** Page

1.1 Numerical simulation and fitting to the microscopic model S3

**2. Supporting Figures**

2.1 Supporting Figure S1 S5

2.2 Supporting Figure S2 S6

2.3 Supporting Figure S3 S7

2.4 Supporting Figure S4 S8

**3. Supporting Tables**

3.1 Supporting Table S1 S10

3.2 Supporting Table S2 S11

3.3 Supporting Table S3 S12

3.4 Supporting Table S4 S13

3.5 Supporting Table S5 S14

# 1. Supporting Methods

## 1.1 Numerical simulation and fitting to the microscopic model

The observed decays for the *T*-range, 203-219 K, were fitted to the 3-state, 2-step microscopic kinetic model (Scheme S1), where $\mathbf{S_1^{\bullet}}$, $\mathbf{S_2^{\bullet}}$ and **P** are states, and $k_{12}$, $k_{21}$ and $k_P$ are first-order rate constants. The fitting was performed by using programs written in Matlab.

$$S_1^{\bullet} \underset{k_{21}}{\overset{k_{12}}{\rightleftharpoons}} S_2^{\bullet} \xrightarrow{k_P} P \qquad \text{Scheme S1}$$

The 3-state, 2-step model was solved symbolically by using the *dsolve* function in the Matlab suite. The following set of ordinary differential equations describe the time dependence of $\mathbf{S_1^{\bullet}}$, $\mathbf{S_2^{\bullet}}$ and **P**:

$$dS_1/dt = -k_{12} * S_1 + k_{21} * S_2 \qquad \text{Eq. SI-1}$$

$$dS_2/dt = k_{12} * S_1 - k_{21} * S_2 - k_p * S_2 \qquad \text{Eq. SI-2}$$

$$dP/dt = k_p * S_2 \qquad \text{Eq. SI-3}$$

The equations were solved explicitly, under the initial conditions, $S_1 = A_1$, $S_2 = 1\text{-}A_1$ and $P = 0$, where $A_1$ is the initial concentration of the $S_1$ state,.

The substrate radical signal decays to zero and concommitantly forms diamagnetic products. Therefore, the solution for $P(t)$ was fit to the inverse of the substrate radical decay curve by using the least squares regression analysis equation:

$$\min_{x} ||F(x, xdata) - ydata||_2^2 = \sum_i (F(x, xdata\ a_i) - ydata\ a_i)^2 \qquad \text{Eq. SI-4}$$

In Eq. SI-4, $x$ is the set of variables $k_{12}$, $k_{21}$, $k_p$ and $A_1$. The *xdata* and *ydata* are the time and substrate radical amplitude matricies for the decay curve, respectively. The *lsqcurvefit* function in Matlab was used to find the numerical solution for $P(t)$ for each decay. Trust-region-reflective and Levenberg-Marquardt algorithms were used. Both algorithms were shown to have no significant difference between results, with the lower bounds of the step size and the function set to $10^{-10}$.

## 2. Supporting Figures

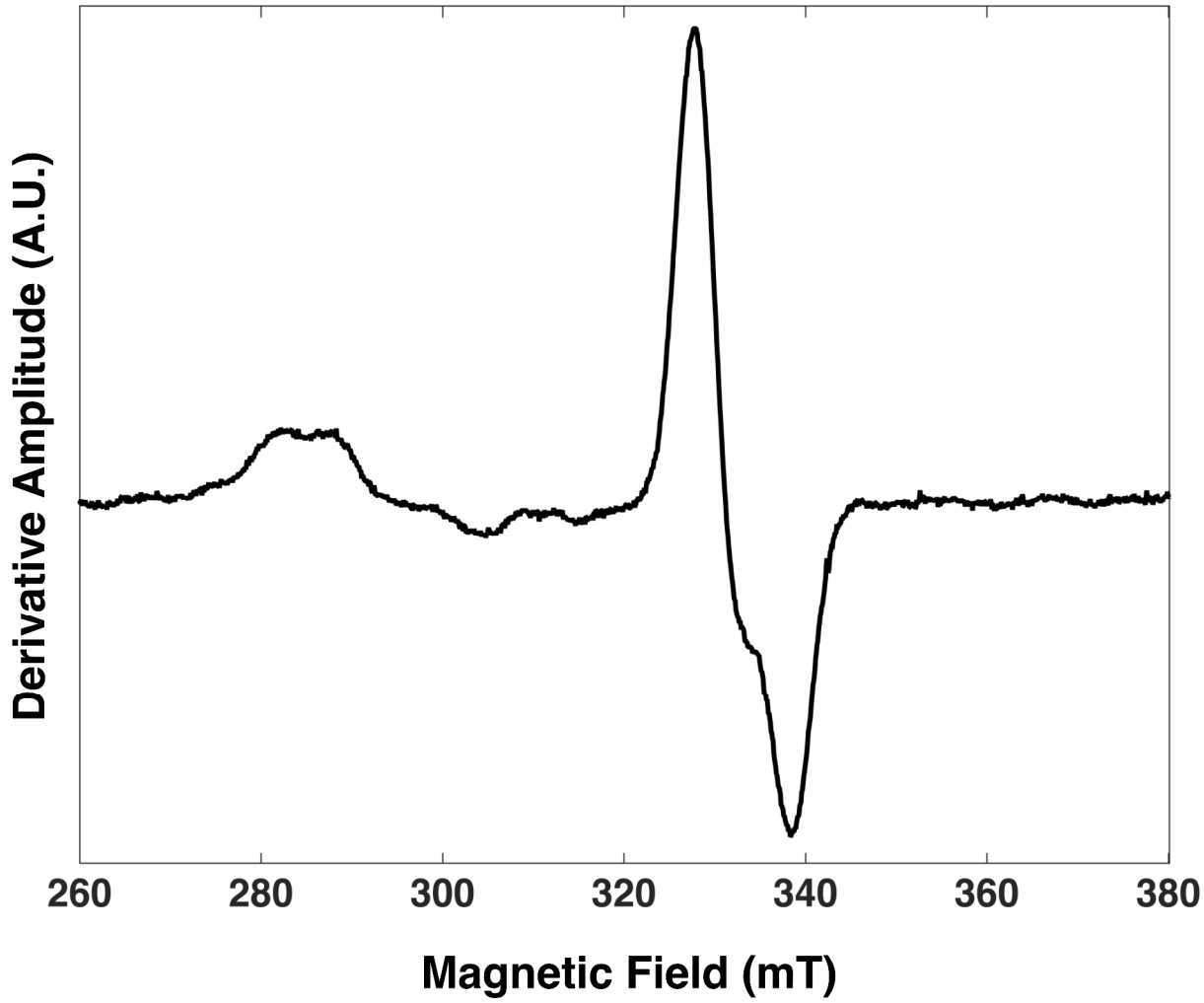


**Figure S1**. **Electron paramagnetic resonance spectrum of the aminoethanol-generated Co(II)-substrate radical pair EPR spectrum in EAL**. *EPR conditions*: microwave frequency, 9.3405 GHz; microwave power, 20 mW; magnetic field modulation, 1.0 mT; modulation frequency, 100 kHz; temperature, 207 K; single scan.

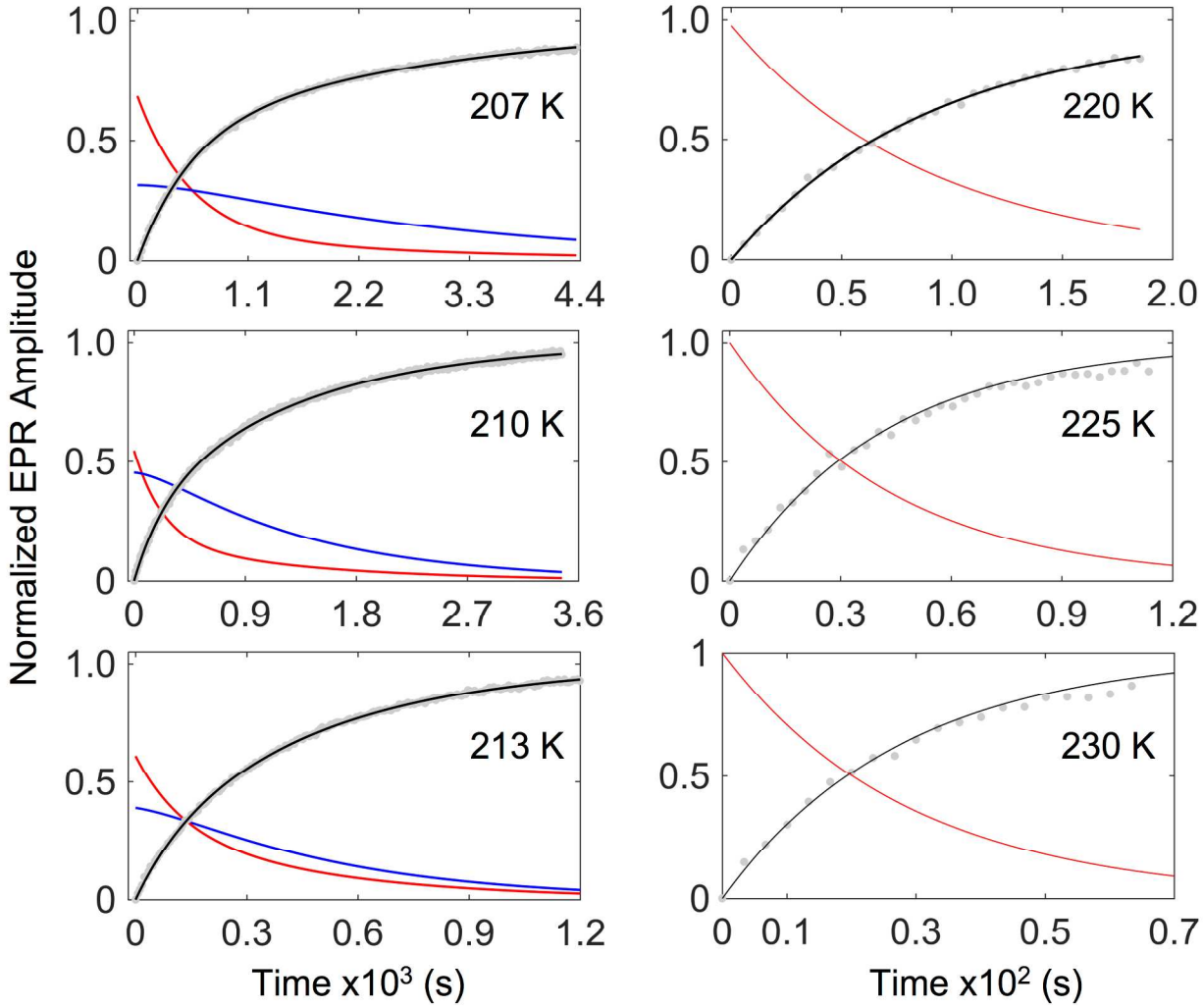


**Figure S2. Numerical simulations of the amplitude *versus* time data at different *T* values.** Simulations are based on the 3-state, 2-step mechanism and the set of coupled differential equations for the time-dependence of the $\mathbf{S_1}^{\bullet}$, $\mathbf{S_2}^{\bullet}$, and **P** populations. The time-dependence of the product (**P**) growth represents unity minus the normalized, measured substrate radical decay, as obtained from the EPR amplitudes, and is shown as light grey circles. The simulated **P** growth curve is shown as a black line. The decay of the $\mathbf{S_1}^{\bullet}$ and $\mathbf{S_2}^{\bullet}$ states is shown by the red and blue curves, respectively. At $T \geq 220$ K, the single $\mathbf{S}^{\bullet}$ state decays with first-order kinetics to **P** (red curve only).

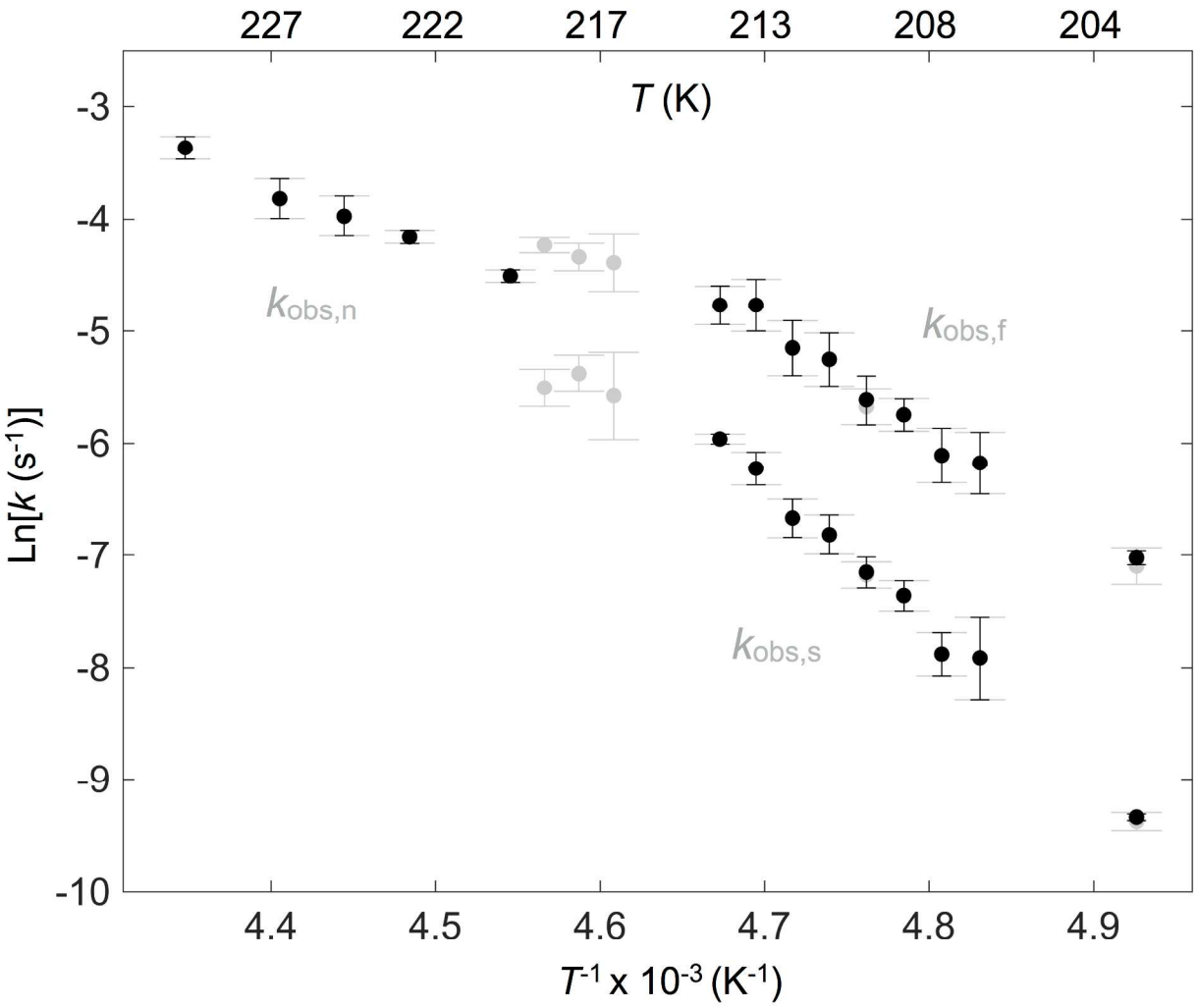


**Figure S3. Comparison of the rate constants from the empirical fitting of the substrate radical decay data (grey circles, grey labels) with the rate constants obtained by fitting the numerical simulation of the time-dependence of the substrate radical decay.** Empirical mono- and bi-exponential fitting of the substrate radical decay data (grey circles, grey labels); mono- and biexponential rate constants obtained by fitting the numerical simulation (black circles). The numerical simulation was based on the model in Scheme S1. The error bars represent the standard deviation for simulations of at least three separate decay measurements.

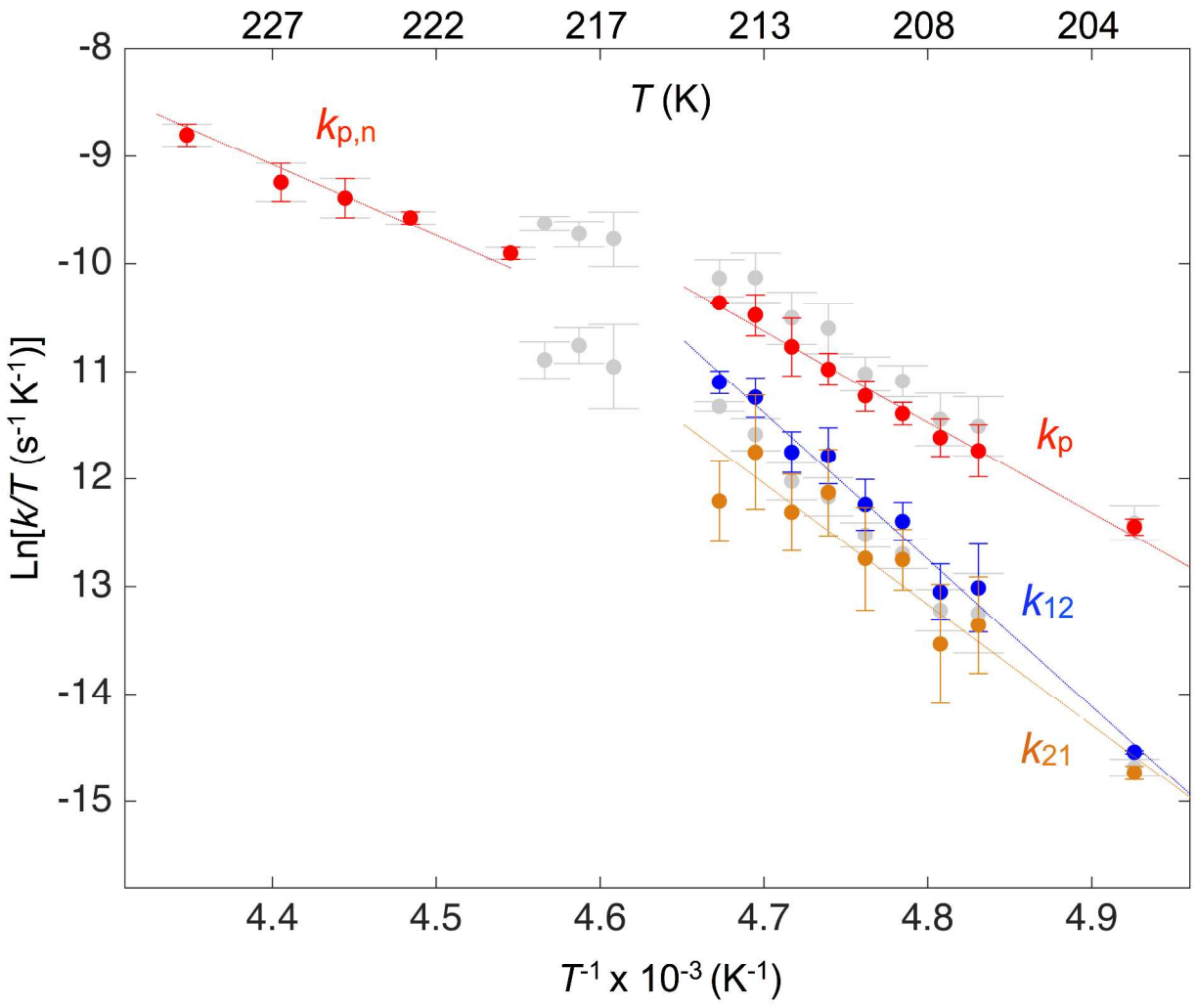


**Figure S4. Eyring plot of the low-temperature native, $k_n$, and microscopic rate constants, $k_{12}$, $k_{21}$ and $k_P$, obtained from the kinetic simulations of the substrate radical EPR signal decay**. The microscopic rate constants are overlaid on the observed mono- and bi-exponential rate constants obtained from the empirical fit to the substrate radical EPR signal decay (light grey circles). The mean $k$ values for each temperature are shown, and error bars represent the standard deviation for at least three separate decay measurements.

## 3. Supporting Tables

**Table S1. Observed first-order rate constant and normalized amplitude parameters for the fit of the mono- and biexponential functions to the $Co^{2+}$-substrate radical pair decay kinetics at different temperatures.**[a]

| $T$ (K) | $k_{obs,n}$ ($s^{-1}$)[b] | $A_{obs,n}$ | $k_{obs,f}$ ($s^{-1}$) | $A_{obs,f}$ | $k_{obs,s}$ ($s^{-1}$) | $A_{obs,s}$ | $R^2$ [c] |
|---|---|---|---|---|---|---|---|
| 203 | -- | -- | $8.3(\pm1.4)\times10^{-4}$ | $0.60\pm0.03$ | $8.5(\pm0.07)\times10^{-5}$ | $0.40\pm0.03$ | 0.9978 |
| 207 | -- | -- | $2.1(\pm0.7)\times10^{-3}$ | $0.46\pm0.16$ | $3.7(\pm1.6)\times10^{-4}$ | $0.54\pm0.16$ | 0.9993 |
| 208 | -- | -- | $2.2(\pm0.6)\times10^{-3}$ | $0.49\pm0.12$ | $3.8(\pm0.8)\times10^{-4}$ | $0.51\pm0.12$ | 0.9988 |
| 209 | -- | -- | $3.2(\pm0.5)\times10^{-3}$ | $0.38\pm0.08$ | $6.4(\pm0.1)\times10^{-4}$ | $0.62\pm0.08$ | 0.9992 |
| 210 | -- | -- | $3.4(\pm0.6)\times10^{-3}$ | $0.39\pm0.07$ | $7.6(\pm0.1)\times10^{-4}$ | $0.61\pm0.07$ | 0.9992 |
| 211 | -- | -- | $5.2(\pm1.4)\times10^{-3}$ | $0.30\pm0.15$ | $1.1(\pm0.2)\times10^{-3}$ | $0.70\pm0.15$ | 0.9986 |
| 212 | -- | -- | $5.8(\pm1.6)\times10^{-3}$ | $0.33\pm0.13$ | $1.3(\pm0.2)\times10^{-3}$ | $0.67\pm0.13$ | 0.9993 |
| 213 | -- | -- | $8.5(\pm2.2)\times10^{-3}$ | $0.30\pm0.13$ | $2.0(\pm0.3)\times10^{-3}$ | $0.70\pm0.13$ | 0.9992 |
| 214 | -- | -- | $8.5(\pm1.6)\times10^{-3}$ | $0.32\pm0.10$ | $2.6(\pm0.1)\times10^{-3}$ | $0.68\pm0.10$ | 0.9993 |
| 217 | -- | -- | $1.2(\pm0.4)\times10^{-2}$ | $0.63\pm0.09$ | $3.8(\pm1.8)\times10^{-3}$ | $0.37\pm0.09$ | 0.9990 |
| 218 | -- | -- | $1.3(\pm0.2)\times10^{-2}$ | $0.56\pm0.09$ | $4.6(\pm0.8)\times10^{-3}$ | $0.44\pm0.09$ | 0.9953 |
| 219 | -- | -- | $1.4(\pm0.1)\times10^{-2}$ | $0.62\pm0.12$ | $4.1(\pm0.7)\times10^{-3}$ | $0.38\pm0.12$ | 0.9945 |
| 220 | $1.1(\pm0.1)\times10^{-2}$ | $1.00\pm0.00$ | -- | -- | -- | -- | 0.9978 |
| 223 | $1.6(\pm0.1)\times10^{-2}$ | $1.00\pm0.00$ | -- | -- | -- | -- | 0.9982 |
| 225 | $1.9(\pm0.4)\times10^{-2}$ | $1.00\pm0.00$ | -- | -- | -- | -- | 0.9748 |
| 227 | $2.2(\pm0.4)\times10^{-2}$ | $1.00\pm0.00$ | -- | -- | -- | -- | 0.9450 |
| 230 | $3.5(\pm0.4)\times10^{-2}$ | $1.00\pm0.00$ | -- | -- | -- | -- | 0.9460 |

[a]Mean values and standard deviations correspond to at least three separate determinations ($n$=3).
[b]Fit includes $k_{cat}$ values data from 277 K [$5.7(\pm0.4)\times10^{0}$ $s^{-1}$] and 295 K [$2.9(\pm0.2)\times10^{1}$ $s^{-1}$].
[c]$R$ is Pearson's correlation coefficient.

**Table S2. First-order microscopic rate constant and amplitude parameters for the $Co^{2+}$-substrate radical pair decay kinetics at different temperatures, obtained by simulation by using the 3-state, 2-step model.[a]**

| $T$ (K) | $[S\bullet]_0$ | $[S\bullet_1]_0$ | $k_{21}$ ($s^{-1}$) | $k_{12}$ ($s^{-1}$) | $[S\bullet_2]_0$ | $k_p$ or $k_{p,n}$ ($s^{-1}$)[b, c] | $R^2$[d] |
|---|---|---|---|---|---|---|---|
| 203 | -- | 0.28±0.04 | 8.1(±0.5) ×$10^{-5}$ | 9.8(±0.01) ×$10^{-5}$ | 0.72±0.04 | 8.0(±0.6) ×$10^{-4}$ | 0.9630 |
| 207 | -- | 0.31±0.13 | 3.3(±1.8) ×$10^{-4}$ | 4.6(±2.3) ×$10^{-4}$ | 0.69±0.13 | 1.7(±0.5) ×$10^{-3}$ | 0.9884 |
| 208 | -- | 0.33±0.07 | 2.8(±2.0) ×$10^{-4}$ | 4.5(±1.3) ×$10^{-4}$ | 0.67±0.07 | 1.9(±0.4) ×$10^{-3}$ | 0.9644 |
| 209 | -- | 0.33±0.04 | 6.0(±2.0) ×$10^{-4}$ | 8.6(±1.6) ×$10^{-4}$ | 0.67±0.04 | 2.4(±0.3) ×$10^{-3}$ | 0.9790 |
| 210 | -- | 0.35±0.06 | 6.1(±3.7) ×$10^{-4}$ | 1.0(±0.3) ×$10^{-3}$ | 0.65±0.06 | 2.8(±0.4) ×$10^{-3}$ | 0.9512 |
| 211 | -- | 0.37±0.10 | 1.1(±0.6) ×$10^{-3}$ | 1.6(±0.5) ×$10^{-3}$ | 0.63±0.10 | 3.6(±0.6) ×$10^{-3}$ | 0.9742 |
| 212 | -- | 0.37±0.13 | 9.5(±4.0) ×$10^{-4}$ | 1.7(±0.3) ×$10^{-3}$ | 0.63±0.13 | 4.4(±1.4) ×$10^{-3}$ | 0.9899 |
| 213 | -- | 0.36±0.07 | 1.7(±1.2) ×$10^{-3}$ | 2.8(±0.6) ×$10^{-3}$ | 0.64±0.07 | 6.0(±1.3) ×$10^{-3}$ | 0.9906 |
| 214 | -- | 0.33±0.06 | 1.1(±0.5) ×$10^{-3}$ | 3.2(±0.4) ×$10^{-3}$ | 0.67±0.06 | 6.7(±0.04) ×$10^{-3}$ | 0.9950 |
| 220 | 1.00±0.00 | -- | -- | -- | -- | 1.1(±0.1) ×$10^{-2}$ | 0.9978 |
| 223 | 1.00±0.00 | -- | -- | -- | -- | 1.6(±0.1) ×$10^{-2}$ | 0.9982 |
| 225 | 1.00±0.00 | -- | -- | -- | -- | 1.9(±0.4) ×$10^{-2}$ | 0.9748 |
| 227 | 1.00±0.00 | -- | -- | -- | -- | 2.2(±0.4) ×$10^{-2}$ | 0.9450 |
| 230 | 1.00±0.00 | -- | -- | -- | -- | 3.5(±0.4) ×$10^{-2}$ | 0.9460 |

[a]Mean values and standard deviations correspond to at least three separate determinations ($n$=3).
[b]$k_p$, 203-214 K; $k_{p,n}$, 220-230 K
[c]Fit for $k_{p,n}$ includes $k_{cat}$ data from 277 K [5.7(±0.4) ×$10^0$ $s^{-1}$] and 295 K [2.9(±0.2) ×$10^1$ $s^{-1}$].
[d]$R$ is Pearson's correlation coefficient.

**Table S3. Arrhenius reaction rate parameters for the microscopic rate constants of the $Co^{2+}$-substrate radical pair decay**.[a]

| Rate Constant | $\ln[A_{app}\ (s^{-1})]$ | $E_{a,app}$ (kcal $mol^{-1}$) | $R^{2\,b}$ |
|---|---|---|---|
| $k_{21}$ | 47.1 (±6.8) | 22.7 (±2.8) | 0.9148 |
| $k_{12}$ | 59.2 (±3.3) | 27.6 (±1.4) | 0.9855 |
| $k_p$[c] | 35.4 (±1.6) | 17.2 (±0.7) | 0.9906 |
| $k_{p,n}$[d] | 26.6 (±0.4) | 13.7 (±0.2) | 0.9992 |

[a]Values and standard deviations correspond to linear fits of results in Arrhenius plot of data, Figure 5.
[b]$R$ is Pearson's correlation coefficient.
[c]$k_p$ is the rate constant for $T \leq 214$ K.
[d]$k_{p,n}$ is the rate constant for $T \geq 220$ K.

**Table S4. Activation enthalpy and entropy values obtained from Eyring analysis of the microscopic rate constants**.[a]

| Rate Constant | $\Delta S^{\ddagger}$ (cal mol$^{-1}$ K$^{-1}$) | $\Delta H^{\ddagger}$ (kcal mol$^{-1}$) |
|---|---|---|
| $k_{21}$ | 33.6 (±13.6) | 22.3 (±2.9) |
| $k_{12}$ | 57.6 (±6.6) | 27.1 (±1.4) |
| $k_p$ [a] | 10.2 (±3.1) | 16.7 (±0.6) |
| $k_{p,n}$ [b] | -7.3 (±0.8) | 13.2 (±0.2) |

[a]Values and standard deviations correspond to linear fits of results in Eyring plot, Figure S4.
[b]$k_p$ is the rate constant for $T \leq 214$ K.
[c]$k_{p,n}$ is the rate constant for $T \geq 220$ K.

**TABLE S5.** Values of the 95% confidence intervals (CI) for empirical fits of monoexponential and biexponential functions to the $Co^{II}$-substrate radical pair decay kinetics at different temperatures. The average 95% CI for fits to the ≥3 experimental decays at each temperature are given by the bold-font range in parentheses, following the average best-fit $k_{obs}$ - and $A_{obs}$-values.

| $T$ (K) | $k_{obs,n}$ ($s^{-1}$) | $A_{obs,n}$ | $k_{obs,f}$ ($s^{-1}$) | $A_{obs,f}$ | $k_{obs,s}$ ($s^{-1}$) | $A_{obs,s}$ [a] | $R^2$ [b] |
|---|---|---|---|---|---|---|---|
| 203 | -- | -- | 8.3(±**0.1**) ×$10^{-4}$ | 0.60±**0.01** | 8.5(±**0.1**) ×$10^{-5}$ | 0.40±**0.01** | 0.9978 |
| 207 | -- | -- | 2.1(±**0.05**) ×$10^{-3}$ | 0.46±**0.01** | 3.7(±**0.07**) ×$10^{-4}$ | 0.54±**0.01** | 0.9993 |
| 208 | -- | -- | 2.2(±**0.05**) ×$10^{-3}$ | 0.49±**0.01** | 3.8(±**0.08**) ×$10^{-4}$ | 0.51±**0.01** | 0.9988 |
| 209 | -- | -- | 3.2(±**0.09**) ×$10^{-3}$ | 0.38±**0.01** | 6.4(±**0.07**) ×$10^{-4}$ | 0.62±**0.01** | 0.9992 |
| 210 | -- | -- | 3.4(±**0.1**) ×$10^{-3}$ | 0.39±**0.01** | 7.6(±**0.1**) ×$10^{-4}$ | 0.61±**0.01** | 0.9992 |
| 211 | -- | -- | 5.2(±**0.3**) ×$10^{-3}$ | 0.30±**0.01** | 1.1(±**0.2**) ×$10^{-3}$ | 0.70±**0. 01** | 0.9986 |
| 212 | -- | -- | 5.8(±**0.3**) ×$10^{-3}$ | 0.33±**0.01** | 1.3(±**0.2**) ×$10^{-3}$ | 0.67±**0. 01** | 0.9993 |
| 213 | -- | -- | 8.5(±**0.6**) ×$10^{-3}$ | 0.30±**0.02** | 2.0(±**0.05**) ×$10^{-3}$ | 0.70±**0.02** | 0.9992 |
| 214 | -- | -- | 8.5(±**0.1**) ×$10^{-3}$ | 0.32±**0.06** | 2.6(±**0.1**) ×$10^{-3}$ | 0.68±**0.06** | 0.9993 |
| 217 | -- | -- | 1.2(±**0.1**) ×$10^{-2}$ | 0.63±**0.13** | 3.8(±**0.6**) ×$10^{-3}$ | 0.37±**0.13** | 0.9990 |
| 218 | -- | -- | 1.3(±**0.1**) ×$10^{-2}$ | 0.56±**0.09** | 4.6(±**0.5**) ×$10^{-3}$ | 0.44±**0.09** | 0.9953 |
| 219 | -- | -- | 1.4(±**0.1**) ×$10^{-2}$ | 0.62±**0.06** | 4.1(±**0.4**) ×$10^{-3}$ | 0.38±**0.06** | 0.9945 |
| 220 | 1.1(±**0.02**) ×$10^{-2}$ | 1.00±0.00 | -- | -- | -- | -- | 0.9978 |
| 223 | 1.6(±**0.04**) ×$10^{-2}$ | 1.00±0.00 | -- | -- | -- | -- | 0.9982 |
| 225 | 1.9(±**0.08**) ×$10^{-2}$ | 1.00±0.00 | -- | -- | -- | -- | 0.9748 |
| 227 | 2.2(±**0.2**) ×$10^{-2}$ | 1.00±0.00 | -- | -- | -- | -- | 0.9450 |
| 230 | 3.5(±**0.2**) ×$10^{-2}$ | 1.00±0.00 | -- | -- | -- | -- | 0.9460 |